Inter-Research Science Publisher

Marine Ecology Progress Series
Volume 753:85–104

Published January 30, 2025
https://doi.org/10.3354/meps14777

Presence or absence of a planktonic egg and larval stage affects the intertidal recruitment of *Littorina* species (Gastropoda) during very strong El Niño events

Elizabeth G. Boulding[1,2,*]

[1]Department of Integrative Biology, University of Guelph, Guelph, ON N1G 1W8, Canada
[2]Bamfield Marine Sciences Centre, Bamfield, BC V0R 1B0, Canada

ABSTRACT: Life history traits affecting dispersal ability could affect species' responses to climate change. Size-specific abundances of 4 NE Pacific *Littorina* snail species (2 with planktonic eggs and larvae [planktonic development, PD] and 2 with direct development [DD] from attached egg masses) were compared on 2 rocky intertidal sites near Bamfield on Vancouver Island, British Columbia, Canada, between 1994 and 2021. Two very strong El Niño – Southern Oscillation events (1997/1998 and 2015/2016) were followed by large, significant increases in recruitment of 2 PD species. By contrast, the juvenile recruitment of the common DD species showed varied responses to the first event and a large, significant decrease during the second event. Four hypotheses explaining the effect of the developmental mode on recruitment after very strong El Niño events were evaluated. Two of these hypotheses, (H_1) interspecific competition and (H_2) selective predation of the thin-shelled DD species by a temporarily invading lined shore crab from southern Oregon, USA, were rejected. Alternative hypotheses were that the larval supply and/or juvenile survival of the PD species increased because of (H_3) higher summer sea surface temperature (SST) or (H_4) stronger winter poleward currents and higher minimum winter SST. H_4 was strongly supported by the significant positive 'slope' coefficients for the covariate 'previous February SST' within multivariate autoregressive state-space models of the July and December juvenile PD count anomalies. The northward winter Davidson surface current is faster and warmer during very strong El Niño events, which may increase the larval transport and subsequent intertidal recruitment of the PD species.

KEY WORDS: Abundance patterns · California Current · Coastal Kelvin wave · Direct development · Larval transport · Long-term data series · Sea surface temperature · Time-series modelling

1. INTRODUCTION

Extreme oceanographic and climate events, such as strong El Niño events and marine heat waves, can affect the recruitment of intertidal species with and without a planktonic larval stage, but the mechanisms are not well understood (Navarrete et al. 2002, Broitman et al. 2008, Pfaff et al. 2011, Little et al. 2021, Wethey & Woodin 2022). El Niño events along Northeastern Pacific shores can cause relaxation or reversal (Dudas et al. 2009) of upwelling-favourable winds that usually blow towards the equator in summer (Huyer & Smith 1985, Huyer et al. 2002). These wind relaxations or reversals can generate warmer, downwelling currents with onshore flows that can facilitate the return of competent larvae to the intertidal zone (Farrell et al. 1991, Connolly & Roughgarden 1999, Lundquist et al. 2000, Navarrete et al. 2002, Poulin et al. 2002, Narváez et al. 2006, Broitman et al. 2008, Dudas et al. 2009). Larval behaviour may also affect the extent to which different species are advected onshore (Shanks 1985, 1995, Meyer et al. 2021).

The local arrival of warm coastal Kelvin waves, which form after the equatorial El Niño Kelvin waves reach South America, can be identified within days by

*Corresponding author: boulding@uoguelph.ca

Publisher: Inter-Research · www.int-res.com

local increases in sea surface height and sea surface temperature (SST) (Allen & Hsieh 1997). These poleward Kelvin waves cause the winter poleward flow of the Davidson current along the NE Pacific coastline (Reid & Schwartzlose 1962, Thomson & Krassovski 2010) to become warmer and stronger (Kosro 2002, W. T. Peterson et al. 2017, Zaba et al. 2020, Ray et al. 2022). The warmer and faster Davidson current transports fishes and crustacean larvae thousands of kilometres northward, causing temporary northern range expansions (Pearcy & Schoener 1987, Sorte et al. 2001, Wonham & Hart 2018, Boulding et al. 2020). The 1997/1998 El Niño-enhanced Davidson current caused large permanent range expansions of the invasive European green crab *Carcinus maenas* by transporting its planktonic larvae more than 1000 km north from its NE Pacific site of introduction within a few months (Behrens Yamada & Kosro 2010, Behrens Yamada et al. 2015, 2021). However, the relative roles of marine heat waves and very strong El Niño events in generating recruitment variability of intertidal gastropods with a planktonic larval stage is not well understood (Merlo et al. 2018, Sanford et al. 2019).

Wave-exposed rocky intertidal invertebrates with a planktotrophic larval phase have potential dispersal rates several orders of magnitude greater than similar species without a planktonic larval phase (Kelly & Palumbi 2010). A good example is the northern temperate gastropod genus *Littorina* A. Férussac, 1822, which contains 8 species with a planktotrophic larval stage, 9 species with direct development inside a benthic egg mass, and 1 brooding species that releases live juveniles (Reid 1996, Reid et al. 1996, Rolán-Alvarez et al. 2015). Numerous population genetic studies using DNA markers have confirmed that species of *Littorina* with direct development show a more localised population genetic structure than do species with planktotrophic development (Kyle & Boulding 2000, Lee & Boulding 2009, Rolán-Alvarez et al. 2015). Direct-developing *Littorina* species show more local genetically based adaptation in phenotype (Johannesson et al. 1993, Hull et al. 1996, Rolán-Alvarez et al. 1997, 2015, Boulding et al. 2017, Kess et al. 2021) than do planktotrophic species living in similar habitats (Behrens Yamada 1989, Lee & Boulding 2010). Surprisingly for a model genus, few studies have measured recruitment to intertidal *Littorina* populations (Underwood & McFadyen 1983, Boulding & Van Alstyne 1993), especially over long periods (Sergievsky et al. 1997, Petraitis & Dudgeon 2020), and even fewer have compared the recruitment of species with and without a planktotrophic larval stage (Hughes & Roberts 1981).

Multivariate autoregressive state-space (MARSS) models have been used to estimate the sampling (observation) error separately from the natural (state) variation in the size of a population from year to year (Ives et al. 2003, Holmes et al. 2012, Hampton et al. 2013, Tolimieri et al. 2017, Auger-Méthé et al. 2021); this feature is particularly useful here because counts of small juvenile (post-larval) life stages of a species may be less accurate than counts of large adults. MARSS models can also determine whether density dependence (autoregression) or abiotic and biotic covariates best explain temporal and/or spatial changes in the abundances of a single species (Holmes et al. 2021). For example, the relative magnitude of density dependence (autoregressive coefficients) and species interaction covariate coefficients (predation and/or interspecific competition) differed among species of North Atlantic sharks with different life history characteristics (C. Peterson et al. 2017) and therefore might also differ among *Littorina* species with different life histories. Ranking of models based on their fit to a data set, and subsequent statistical inference, is most valid when a small set of multiple hypotheses is generated *a priori* before any modelling is done (Anderson & Burnham 2002, Anderson 2008).

This paper addresses a gap in the literature between 2 hypothesised mechanisms that explain the distribution and abundance of rocky intertidal macroinvertebrates with planktonic larvae. The disturbance hypothesis states that predation (Connell 1961, Paine 1976, 1984, Menge et al. 2016a,b) and extreme abiotic events (Mieszkowska et al. 2021, Hesketh & Harley 2023) can prevent the 'dominant competitor for primary space' (e.g. the California mussel *Mytilus californianus*) from forming a monoculture (Paine 1984). By contrast, the 'supply-side' ecology hypothesis states that whether a competitively dominant intertidal macroinvertebrate (e.g. the acorn barnacle *Balanus glandula*) forms a monoculture depends on the supply of competent larvae that reach the shore (Gaines & Roughgarden 1985, Connolly & Roughgarden 1999). The relative contributions of these 2 classes of mechanisms must be resolved before the future geographic range limits of intertidal species can be estimated (e.g. Cahill et al. 2013, 2014). The supply-side hypothesis may apply to other intertidal species with a prolonged planktonic larval phase. Although female *L. plena* release fertilised egg capsules throughout the year (Chow 1987), recruitment to intertidal populations in northern California, USA, varies between years and occurs mainly in fall and winter, when SE winds are postulated to transport their planktotrophic larvae onshore (Chow 1989).

Six classes of MARSS models, each combined with the same set of subsets of 2 to 6 non-collinear environmental covariates, were initially used to model the seasonal population dynamics of recent recruits of 3 species of intertidal snails between 1993 and 2021. The objective was to determine why the temporal abundance anomalies of juveniles of 2 *Littorina* species with planktotrophic larvae (planktonic development, PD), *L. plena* and *L. scutulata*, varied inversely with those of juveniles of a direct-developing (DD) species, *L. subrotundata*, with attached egg masses and crawl-away larvae. Four *a priori* hypotheses that could explain the inverse recruitment anomaly pattern were evaluated: H_1: interspecific competition between PD and DD *Littorina* species; H_2: higher relative predation of the thin-shelled DD species by the lined shore crab *Pachygrapsus crassipes*, which temporarily invades after very strong El Niño events (Boulding et al. 2020); H_3: negative responses of DD and positive responses of PD species to warm summer SST and air temperature anomalies; and H_4: increased supply of PD larvae during 2 very strong El Niño events because the increased minimum SST and increased poleward flow rates of the winter Davidson current advects larvae north and/or increases the onshore transport of competent larvae.

2. MATERIALS AND METHODS

2.1. Study sites

Semi-annual surveys of *Littorina* populations (Text S1.1 in Supplement 1 at www.int-res.com/articles/suppl/m753p085_supp1.pdf) were conducted between 1993 and 2021 at 2 wave-exposed rocky intertidal sites: Prasiola Point (PP: 48.81710, −125.16964) and Nudibranch Point (NP: 48.815160, −125.175473) on Vancouver Island, British Columbia, Canada (Fig. 1; Figs. S1 & S2 in Supplement 1). PP had 6 and NP had 7 vertical 1 m transects positioned horizontally along the acorn barnacle littoral zone. Each transect had 5 permanent 10 × 10 cm quadrats that were marked with stainless steel screws (Fig. S3). Quadrats were counted once in July (either late July or the first half of August) and once in December (either late December or early January). Counts from early January were classified as the December counts from the previous year.

Counting was done by using forceps to remove all *Littorina* spp. larger than 1.0 mm in shell length from inside each permanent quadrat (Fig. S3). The removed snails were placed in a labelled 150 mm diameter round Petri dish. A cell culture dish was then used to sort each species into size classes, beginning with the 1.5–2.4 mm size class and ending with the largest size class for that species (Table S1 in Supplement 1). The number of individuals of each species in each size class was recorded before the snails were returned to their original quadrat. From 1993 to July 2009, sorting, recording, and replacement was done at the study sites. Beginning in December 2009, the snails from each quadrat were sorted to the species level under a dissecting scope and then returned to their original quadrat.

2.2. Study animals

2.2.1. Snails

Four species of *Littorina* were present in the permanent quadrats. *L. plena* A. Gould, 1849 and *L. scutulata* A. Gould, 1849 sensu stricto (Mastro et al. 1982, Reid et al. 1996), are PD species; females lay floating egg capsules (Murray 1979) which hatch into feeding larvae that swim freely in the plankton for at least 5 wk before settling in the intertidal zone (Hohenlohe 2002). Two species, *L. subrotundata* (P. P. Carpenter, 1864) and *L. sitkana* R. A. Philippi, 1846, are low-spired and DD; females lay attached gelatinous egg masses, and the eggs hatch into crawl-away juveniles (Boulding et al. 1993). To reduce the number of zero snail counts in my time-series data set, I combined counts for each species into 2 size-classes: 'small' (newly recruited juveniles of shell lengths 1.5–3.4 mm) and 'large' (shell length >3.4 mm). I did not include the more wave-protected DD snail species *L. sitkana* in a separate run of the MARSS time-series modelling described below because it was too rare (Table S1) at my wave-exposed sites (PP and NP) to give good results. To maximise the time series length, I combined the counts for the 2 PD species, *L. plena* and *L. scutulata* sensu stricto, into 1 taxon, '*L. scutulata* sensu lato', enabling the use of the field-sorted snail count data set from July 1994 to July 2009, in which the 2 species were not distinguished.

2.2.2. Shore crabs

During the 2 very strong El Niño events (1997–1998 and 2015–2016) in the time series, and for several years afterwards until they died of old age (Text S1.2), I found lined shore crabs *Pachygrapsus crassipes* Randall, 1840, which are known to prey on

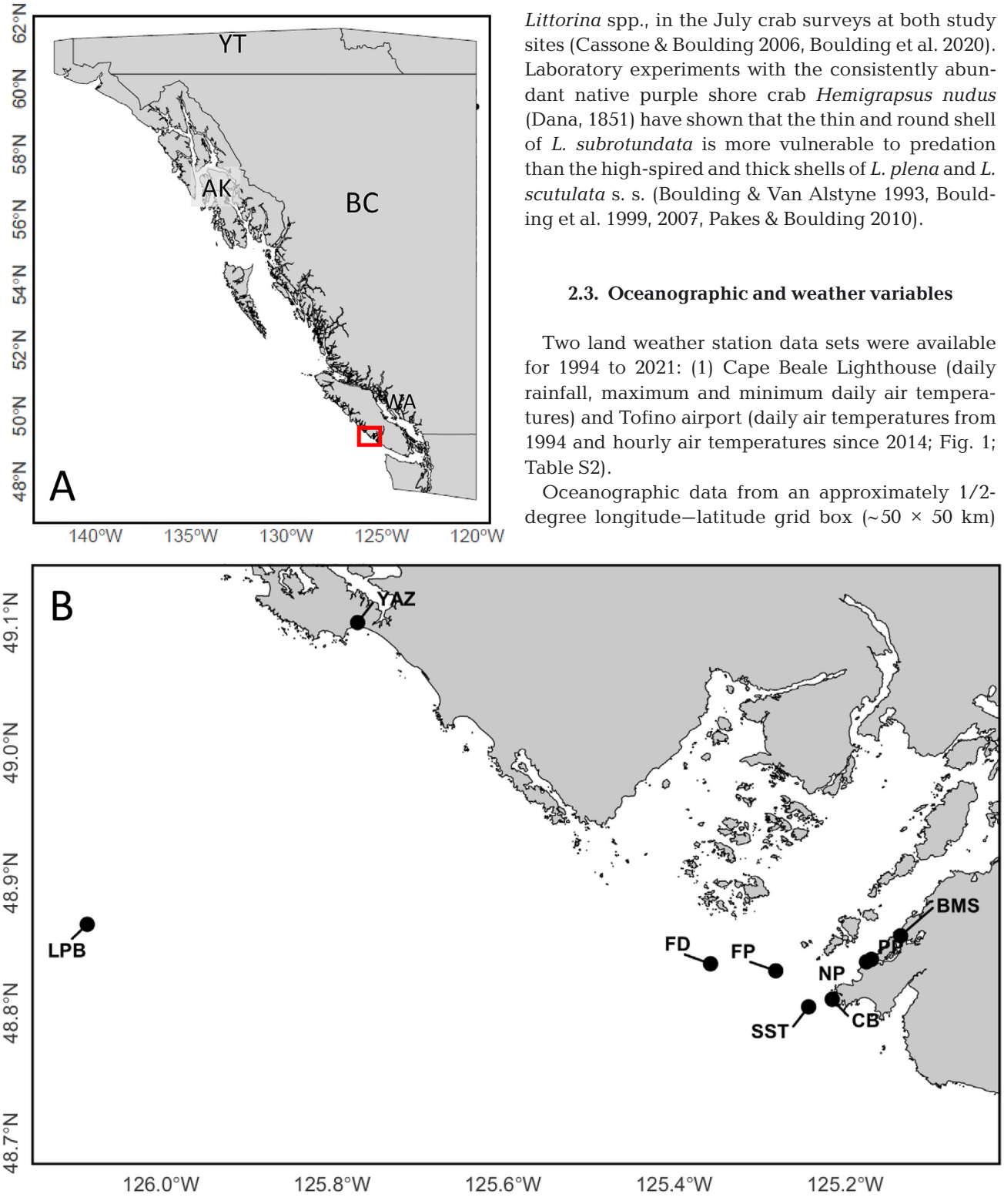

Littorina spp., in the July crab surveys at both study sites (Cassone & Boulding 2006, Boulding et al. 2020). Laboratory experiments with the consistently abundant native purple shore crab *Hemigrapsus nudus* (Dana, 1851) have shown that the thin and round shell of *L. subrotundata* is more vulnerable to predation than the high-spired and thick shells of *L. plena* and *L. scutulata* s. s. (Boulding & Van Alstyne 1993, Boulding et al. 1999, 2007, Pakes & Boulding 2010).

2.3. Oceanographic and weather variables

Two land weather station data sets were available for 1994 to 2021: (1) Cape Beale Lighthouse (daily rainfall, maximum and minimum daily air temperatures) and Tofino airport (daily air temperatures from 1994 and hourly air temperatures since 2014; Fig. 1; Table S2).

Oceanographic data from an approximately 1/2-degree longitude–latitude grid box (~50 × 50 km)

Fig. 1. (A) Low-resolution map of Southern Alaska (AK), British Columbia (BC), Yukon (YT), and Washington (WA) with a red box showing boundaries of the high-resolution map of Barkley Sound, Vancouver Island, BC, Canada shown in panel (B). (B) High-resolution map of study sites, weather stations, and oceanographic climate data: BMS (Bamfield Marine Sciences Centre), CB (Cape Beale Light station weather), FD (Folger Deep Ocean Networks Canada), FP (Folger Pinnacle Ocean Networks Canada), LPB (La Perouse Moored Buoy C46206), NP (Nudibranch Point study site, Second Beach), PP (Prasiola Point study site, Second Beach), SST (latitude and longitude used for NOAA's 1/2-degree oceanographic data products), YAZ (Tofino airport station)

from NOAA's open-ocean satellite databases and models were accessed by selecting a point in the 'blue water' just offshore from the Cape Beale lighthouse with geographical co-ordinates (48.78059, −125.24307) using NOAA NAUPLIUS Step 1 (Table S2). Most of the monthly data sets used here, namely Hadley Sea Surface Temperature, Hadley EN4 Sea Surface Salinity at 5 m (Salinity), International Comprehensive Ocean-Atmosphere Data Set (ICOADS) scaler surface wind speed, and Oceanic Niño index (ONI), were available for the requested baseline of 1992–2021. However, NASA combination-satellite chlorophyll was only available for 1998–2021 (Table S2).

Oceanographic data from the moored 'weather' Buoy C46206 – La Perouse Bank (Fig. 1) provided daily SST, maximum wave height, and windspeed for 1994–2021, with some gaps resulting from technical malfunctions (Table S2). Two other oceanographic data sets were not available for the entire time series from 1994 to 2021 and therefore could not be included in the MARSS modelling: (1) subsurface seawater temperatures from the Ocean Networks Canada (ONC) cable observatories at Folger Deep (depth 100 m, from 2009 to 2021) and Folger Pinnacle (depth 25 m, from 2013 to 2021) at the entrance to Trevor channel (Fig. 1; Table S2, Fig. S2). Surface current direction and speed averaged for January and for July from 2012 to 2021 were from the closest open-ocean High Frequency Radar Stations at Westport State Park, WA (46.9027°, −124.1316°), and Loomis Lake, OR (46.4333°, −124.0589°) (Table S2).

2.4. Transformation of response variables and predictor covariates

The Interactive Spatiotemporal Data & Time Series Toolkit Time-series Explorer, hosted by NOAA: 'COPEPODITE Step 2' (Table S2) was used to calculate and visualise monthly anomalies from the monthly buoy and weather and snail data sets that had been compiled for this study (Fig. 1; Table S2). Also uploaded were my raw snail count data sets. The resulting COPEPODITE Multi-Variable Comparison & Correlation plots were used to check for data problems. The monthly anomalies for NOAA's oceanographic products corresponding to the latitude and longitude of the blue water 'point' that I selected off Cape Beale (SST in Fig. 1), as well as for the uploaded marine buoy and land weather station measurements, were then downloaded. These downloads also contained the difference and the log10 snail count anomalies for each site and season, which are calculated by subtracting the count for each size-class and species from the long-term mean for that site and season (Text S1.3.1).

2.5. H_1: Testing for negative co-occurrence at the quadrat level

Statistical analysis of raw counts that compared more than one snail species usually resulted in violation of the homogeneity of variance assumption as assessed with Levene's test of equality of error variances. Neither square root transformations nor log transformations made the variances more homogeneous. Consequently, to test for negative co-occurrence, I used SPSS (IBM SPSS Statistics version 29.01) to calculate nonparametric pairwise Spearman rank correlations, ρ, between the PD and DD small snail counts from each quadrat. Pairwise Spearman rank correlations were also used to check for collinearity among Hadley SST and all other environmental covariates. SPSS was also used to run nonparametric Mann-Whitney *U*-tests to compare very strong El Niño years (1997–1998 and 2015–2016) and regular non-El Niño years (2005–2013) both between and within species. For comparisons within a species, raw snail counts could be used. However, because of differences among species in their maximum abundances (Text S2.1), log10 anomalies had to be used to compare PD and DD snails. I used $\alpha = 0.05$ for all statistical tests, but exact probabilities are reported when $p > 0.001$.

2.6. MARSS model class and covariate subset selection

Six classes of MARSS recommended for use with environmental covariates (Holmes et al. 2012, 2023) were initially used (Table S3, Text S1.3.3). Only 2 variates, namely the log count anomalies of small snails of a particular taxon at each of the 2 study sites, were ever included in the same model. Separate models were run for each life history type (PD and DD) by season (July and December) combination, as this greatly improved fit and allowed the incorporation of covariates with different time lags. Subsets of non-collinear covariates that had been identified using stepwise univariate linear regression were used (Text S1.3.2). MARSS outputs from all 6 classes of models for each subset of covariates were saved in separate files for each life history by season combination. The outputs included Akaike's information criterion (Akaike 1978) corrected for small sample size (AICc), which mea-

sures model fit, and the 'slope' coefficient, coefficient standard error, and 95% confidence limits for each covariate in the subset. To find the best-fitting model, the ΔAICc values were calculated as the difference between the AICc value for a particular model and the smallest AICc value observed for a particular subset of covariates for each combination of life history by season. Two summary tables were then made showing the 'slope' coefficients and 95% confidence limits at both sites only for the consistently best model class. The first table showed the subsets of covariates that gave the lowest AICc values for each combination of life history by season. To facilitate the testing of the *a priori* hypotheses H_2–H_4, the 'slope' coefficients from one subset of covariates that fit the PD species well in both seasons, but fit the DD species less well, were used to create a second summary table.

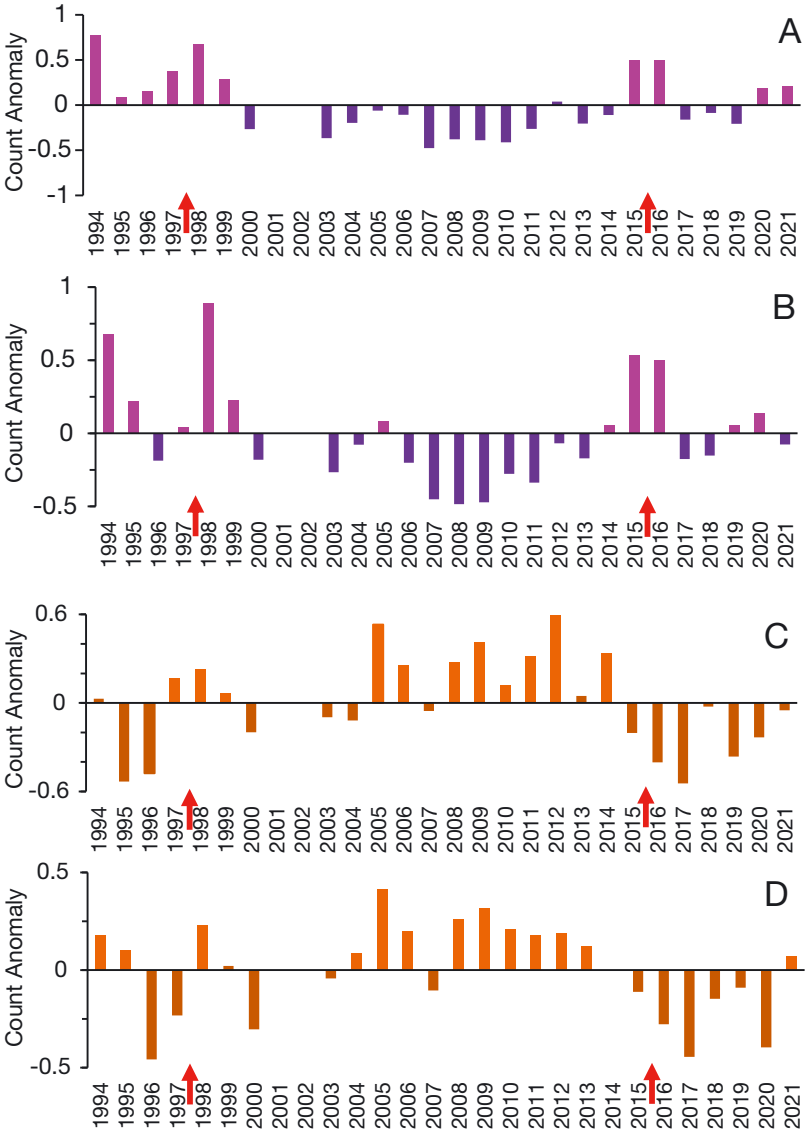

Fig. 2. Annual July anomalies calculated from log10 (x) counts of newly recruited small snails (shell lengths from 1.5 to 3.4 mm), using a 1994–2021 baseline. Red arrows indicate very strong El Niño events from 1997 to 1998 and 2015 to 2016. Magenta positive/purple negative: *Littorina scutulata* sensu lato (*L. scutulata* sensu stricto and *L. plena* combined) = planktotrophic development. Orange positive/brown negative: small *L. subrotundata* = direct development. There was no sampling during July 2002 or July 2003. (A) *L. scutulata* s. l. at Prasiola Point (PP), (B) *L. scutulata* s. l. at Nudibranch Point (NP), (C) *L. subrotundata* at PP, (D) *L. subrotundata* at NP

3. RESULTS

3.1. Effect of life history on population responses to very strong El Niño years

3.1.1. Small snail count anomaly plots

The newly-recruited small snails of the PD species (*Littorina scutulata* s. l.) showed large positive count anomalies during the very strong (ONI > +2.5°C) El Niño in 1997–1998 and 2015–2016. This positive relationship was observed for both the July (logarithmic: Fig. 2A,B, arithmetic: Fig. S4A,B) and for the December (logarithmic: Fig. 3A,B, arithmetic: Fig. S5A,B) sampling periods. The small PD snails also showed a small positive count anomaly in 1994, which may have resulted from the strong El Niño (ONI: > +1.6°C) from January to March 1992.

By contrast, the newly recruited small snails of the DD species showed negative count anomalies during the very strong 2015–2016 El Niño during July (logarithmic: Fig. 2C,D, arithmetic: Fig. S4C,D) and December (logarithmic: Fig. 3C,D, arithmetic: Fig. S5C,D) except the very small positive anomaly at NP in December 2015. The small DD count anomalies were more complex during the 1997–1998 El Niño. The small DD snails showed moderate negative count anomalies at NP in July 1997 (logarithmic: Fig. 2D, arithmetic: Fig. S4D) and very small negative count anomalies at PP and NP in December 1998 (logarithmic: Fig. 3C, arithmetic:

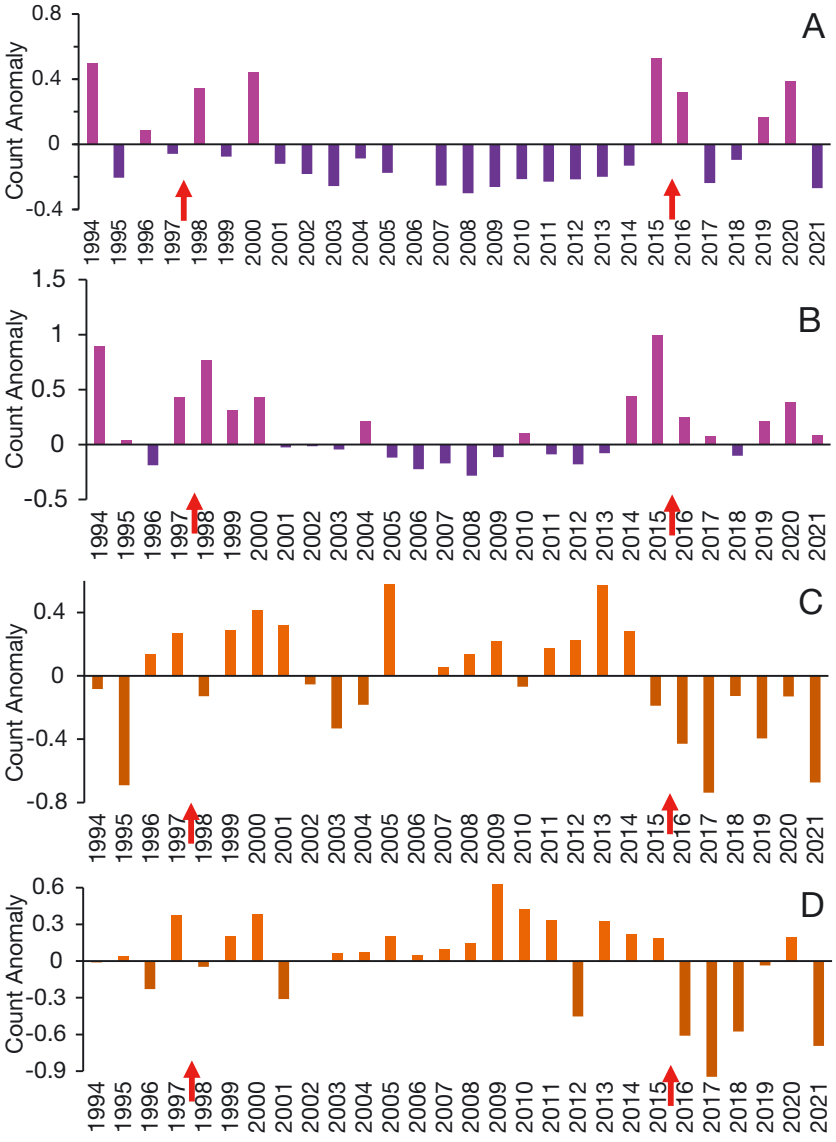

Fig. 3. As in Fig. 2, but for annual December anomalies. There was no sampling during December 2006 at PP. (A) *L. scutulata* s. l. at PP, (B) *L. scutulata* s. l. at NP, (C) *L. subrotundata* at PP, (D) *L. subrotundata* at NP

Fig. S5C). Surprisingly, the small DD snails showed small positive count anomalies at PP in July 1997 and 1998 (logarithmic: Fig. 2C,D, arithmetic: Fig. S4C,D) and small positive count anomalies at both sites in December 1997 (logarithmic: Fig. 3C,D, arithmetic: Fig. S5C,D).

Newly recruited small DD snails were more likely to show large positive count anomalies during regular years without very strong El Niño events, which included July censuses from 2005 to 2013 (logarithmic: Fig. 2C,D, arithmetic: Fig. S4C,D) and December censuses from 2005 to 2014 (logarithmic: Fig. 3C,D, arithmetic: Fig. S5C,D).

By contrast during regular years, small PD snails showed negative log10 anomalies for July censuses during 2000–2014 and 2017–2018 (Fig. 2C,D), and for December (Fig. 3C,D) censuses during 2000–2013, 2017, and 2021, but a positive anomaly in December 2020.

3.1.2. Large snail count anomaly plots

Plots of the large PD snails showed highly significant positive arithmetic count anomalies in both the July (Fig. S6A,B) and the December sampling periods (Fig. S7A,B) during years with a very strong El Niño (1997–1998, 2015, 2016).

By contrast, large DD snails showed negative arithmetic count anomalies during years with a very strong El Niño (1997–1998, 2015, 2016) (Figs. S6C,D & S7C,D). Large DD snail counts were zero inside quadrats at PP in December very strong El Niño years (2015, 2016), and also in 2021 (Fig. S7C). In addition, there was an overall tendency for arithmetic count anomalies for adult DD snails to decline linearly over the study period of 2014–2021, especially for the December counts for NP (Fig. S7D).

3.1.3. Responses to very strong El Niño: between-taxa nonparametric statistics

The mean rank of the log10 anomalies for small PD *L. scutulata* s. l. during the very strong 1997–1998 El Niño event was significantly larger than the mean rank for the log10 anomalies for small DD *L. subrotundata* (nonparametric independent-samples Mann-Whitney *U*-test, N = 8, p = 0.046). Similarly, during the very strong 2015–2016 El Niño event, the mean rank of the log10 anomalies for small *L. scutulata* s. l. was highly significantly larger than the mean rank of the log10 anomalies for *L. subrotundata* (Mann-Whitney *U*-test, N = 8, $p < 0.001$).

By contrast, the DD snails increased in abundance during the years without very strong El Niño events (2005–2013). The mean rank of the 2005–2013 log10 anomalies for small PD snails was significantly smaller than the mean rank of the log10 anomalies for the DD species (Mann-Whitney *U*-test, N = 35, $p < 0.001$).

3.1.4. Responses to very strong El Niño: within-taxon nonparametric statistics

Statistical comparisons within a taxon showed similar patterns. The mean ranks of the raw counts of the small PD snails were significantly larger for the very strong El Niño years (1997–1998 and 2015–2016) than for regular years (2005–2013) for both sites and seasons (Mann-Whitney *U*-test). This was true during July at PP (El Niño mean rank = 584.62 with N = 110, regular years mean rank = 349.14 with N = 655, $p < 0.001$), July at NP (El Niño mean rank = 643.01 with N = 144, regular years mean rank = 418.97 with N = 764, $p < 0.001$), December at PP (El Niño mean rank = 478.10 with N = 140, regular years mean rank = 319.28 with N = 561, $p < 0.001$), and December at NP (El Niño mean rank = 559.29 with N = 173, regular years mean rank = 415.40 with N = 713, $p < 0.001$).

Similar statistical results were obtained for the within-taxon comparison for the large PD snails. The mean rank of the large PD raw counts was highly significantly larger during El Niño years than during regular years. This trend was highly significant for both seasons at both sites (Mann-Whitney *U*-test: PP-December, N = 140, 561, $p < 0.001$; NP-December, N = 173, 713, $p < 0.001$; PP- July, N = 110, 655, $p < 0.001$; NP- July, N = 144, 764, $p < 0.001$).

By contrast, the within-taxon comparison of small snails of the DD species showed the opposite result. The mean ranks of the raw counts within the small DD snails were significantly smaller during El Niño years (1997–1998 and 2015–2016) than in regular years (2005–2013) except in July at PP (Mann-Whitney *U*-tests: July at PP: El Niño mean rank = 358.00 with N = 110, regular year mean rank = 387.20 with N = 655, $p = 0.199$; July at NP: El Niño mean rank = 414.56 with N = 144, regular year mean rank = 462.03 with N = 764, $p = 0.046$; December at PP: El Niño mean rank = 307.76 with N = 140, regular year mean rank = 461.79 with N = 561, $p = 0.005$; December at NP: El Niño mean rank = 392.72 with N = 173, regular year mean rank = 455.82 with N = 713, $p < 0.004$).

Similarly, the raw counts of the large snails of the DD species had significantly higher mean ranks of their raw counts in regular years (2005–2013) relative to El Niño years (1997–1998 and 2015–2016) at both sites in December but not in July at PP (Mann-Whitney *U*-test: PP-December, N = 140, 561, $p < 0.001$; NP-December, N = 173, 713, $p = 0.004$; PP-July, N = 110, 655, $p = 0.258$; NP- July, N = 144, 764, $p = 0.068$). Parametric statistical tests gave very similar results (see Text S2.2).

3.2. H_1: Interspecific competition between small PD and DD *Littorina*

The Spearman rank correlation matrix structure provided no evidence for negative co-occurrence between small PD and DD snails at the quadrat level as predicted under H_1: interspecific competition. Instead, correlations between the density of the wave-exposed DD species and PD species within a particular quadrat were positive for 3 out of 4 life-history-by-site groupings showing positive co-occurrence. Spearman rank correlations between the raw counts for small DD snails (*L. subrotundata*) and those for small PD snails (*L. scutulata* s. l.) were highly significantly positive in July (PP: $\rho = 0.198$, N = 765, $p < 0.001$; NP: $\rho = 0.288$, N = 908, $p < 0.001$) and December at NP 0.230, N = 886, $p < 0.001$) but were not significantly positively correlated in December at PP ($\rho = 0.0456$, N = 701, $p = 0.228$). Snails found in the quadrats during low tide were usually inside a crevice in the rock or touching the plates of the acorn barnacle *Balanus glandula* (Fig. S3). Identical results were obtained when Pearson parametric correlations were used (results not shown).

3.3. Physical and biological covariates correlated with snail recruitment

HF-Radar Network estimates of monthly average current direction showed a significant difference in the deviation of degrees from North ($p = 0.005$) between January and July. The January mean was 299.5°, equivalent to the direction West–Northwest, and the July mean was 188.63°, equivalent to the direction South (Table S4). The maximum January surface current speed observed was 29.6 cm s^{-1} (Table S4).

Hadley SST anomalies were highly significantly positively correlated ($p < 0.001$) with the Reynold's SST, the mean and minimum La Perouse (LP) buoy SST, the mean Tofino air temperature, and the mean

daily-minimum air temperature at the Cape Beale lighthouse anomalies, but were negatively correlated with ICOADS scaler windspeed anomalies (Table S5). Potential covariates that were uncorrelated with Hadley SST anomalies included the anomalies for combined satellite chlorophyll, Hadley_EN4 Salinity 5 m, rainfall at Cape Beale lighthouse, Tofino airport minimum air temperatures, LP buoy windspeed, and LP buoy maximum wave height (Table S5).

A large positive SST anomaly in the previous February, which occurred during very strong El Niño events, was the best predictor of high recruitment of the PD species and low recruitment of the DD species. Newly recruited small snails of the PD species were most abundant at Sites PP and NP, when there was a large positive anomaly in the previous February SST for both July (Fig. 4C) and December (Fig. 4D).

The ONI near equatorial region 3.4 defined 2 very strong El Niño events during the study period, from 1997 to 1998 and from 2015 to 2016, as well as some weaker El Niño events (Fig. 5A). Large numbers of juveniles of the non-indigenous lined shore crab successfully recruited to the 2 Vancouver Island study sites only after the very strong El Niño events (Fig. 5B). Beginning in 2015, lined shore crabs were quantitatively observed (Text S1.2), sexed, and measured at both sites but were confirmed to have disappeared by July 2021 (pers. obs.). By contrast, the count anomaly for the adult large PD snails increased slowly after very strong El Niño events as defined by the ONI (Fig. 5C,D).

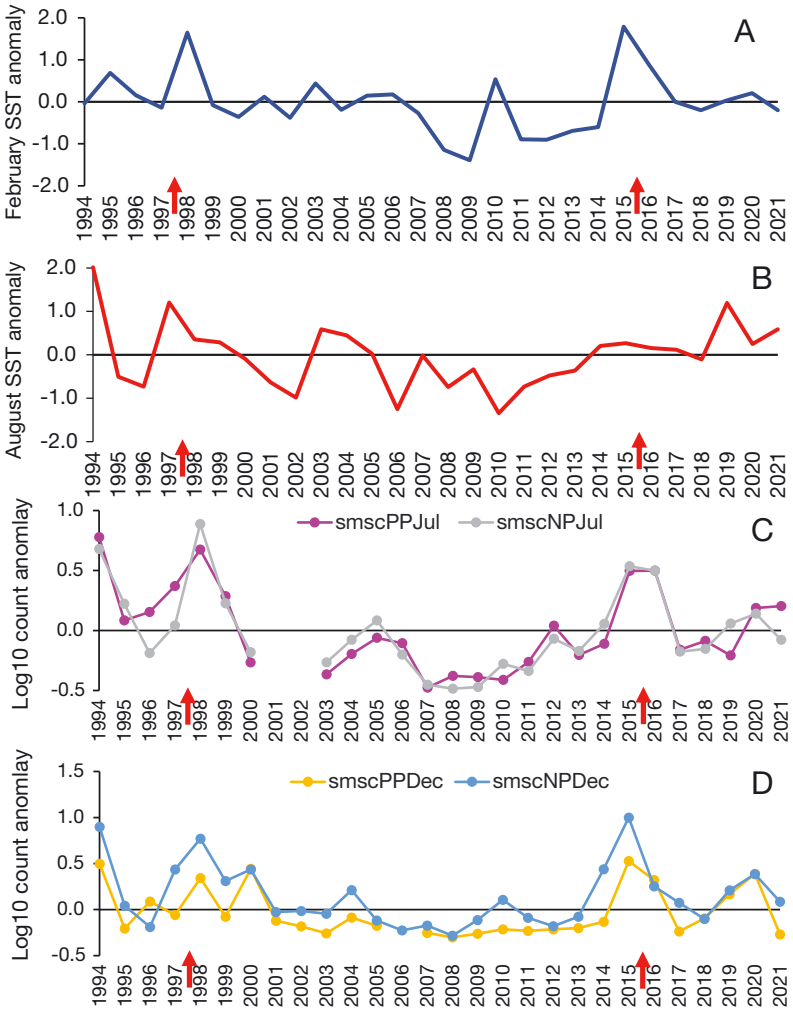

Fig. 4. (A) February Hadley sea surface temperature (SST) anomaly, (B) August Hadley SST anomaly from the same year, (C) July (Jul), and (D) December (Dec) log10 count anomalies of newly recruited small (sm: shell lengths from 1.5 to 3.4 mm) *Littorina scutulata* sensu lato (sc) with planktotrophic development (*L. scutulata* sensu stricto and *L. plena* combined) at the 2 study sites: Prasiola Point (PP) and Nudibranch Point (NP). Red arrows indicate very strong El Niño events from 1997 to 1998 and 2015 to 2016

The Hadley satellite SST and the LP buoy SST monthly means were highly correlated (Table S5), and both showed that the warmest minimum winter SST occurred during very strong El Niño events (Fig. S8A). The increased SST in the 2015–2016 event was followed by an increase in the subsurface sea temperature at 25 m and then by an increase in sea temperature at 95.6 m (Fig. S8B). The transfer of anomalously warm water from the shallow to the deeper layers was more obvious when only the dates for which the ONC data were available for 25 or 95.6 m were plotted (Figs. S9 & S10).

3.4. MARSS model selection

The best fitting of the 6 MARSS model classes to the snail anomalies data set was the state variable process-error-only (Text S2.3) which was a mean-reverting model with initial values of x at time 0 determined by the data matrix (Eq. 1; model 13.4c in Table S3:

$$\mathbf{x}_t = \mathbf{B}_t\mathbf{x}_{t-1} + \mathbf{C}_t\mathbf{c}_t + \mathbf{w}_t, \text{ where } \mathbf{w}_t \sim \text{MVN}(0,\mathbf{Q}_t) \quad (1)$$

where $\mathbf{B}_t$ is a matrix containing autoregressive coefficients for $m \times 1$ state vectors $\mathbf{x}_t$ and $\mathbf{x}_{t-1}$, which estimate the effect of the abundance of each snail species

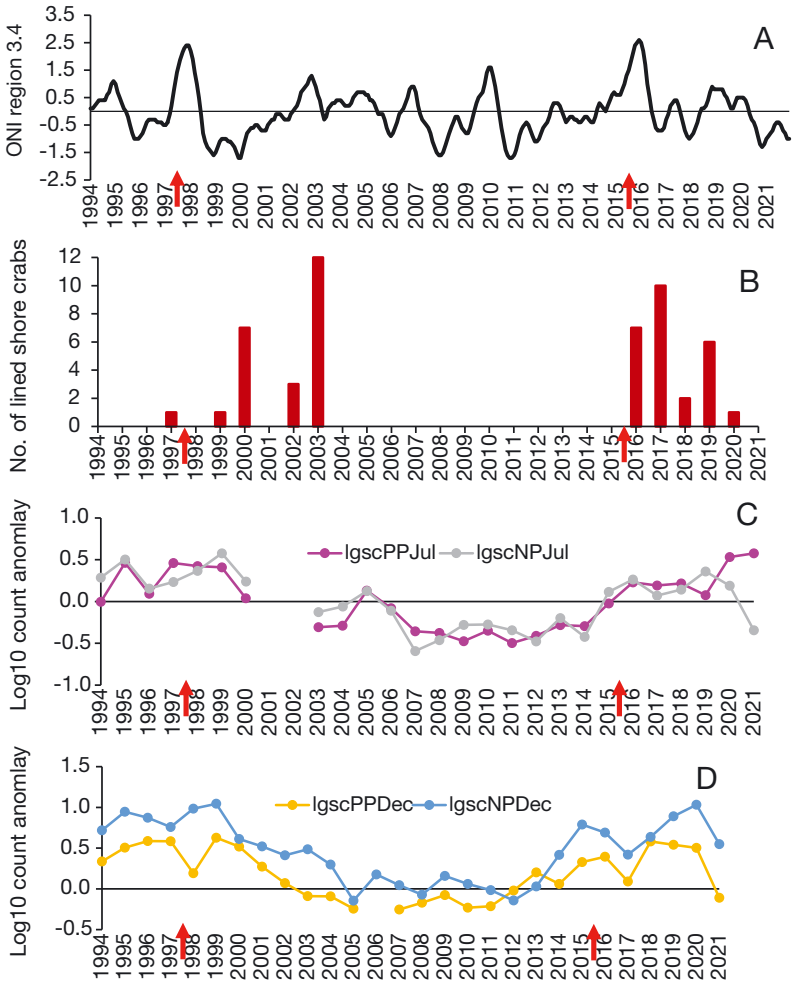

Fig. 5. (A) Oceanic Niño index (ONI) region 3.4 (running average over 3 mo, https://ggweather.com/enso/oni.htm). (B) July counts for the predatory lined shore crab *Pachygrapsus crassipes* during its 2 temporary range extensions to Bamfield from south of Coos Bay, Oregon. (C) July (Jul), and (D) December (Dec) log10 count anomalies of adult (large (lg): shell lengths from 3.5 to 11.0 mm) *Littorina scutulata* sensu lato (sc) with planktotrophic development (*L. scutulata* sensu stricto and *L. plena* combined) at the 2 study sites, Prasiola Point (PP) and Nudibranch Point (NP). Red arrows indicate very strong El Niño events from 1997 to 1998 and 2015 to 2016

at time $t-1$ based on its abundance at time t; $\mathbf{c}_t$ is the $p \times 1$ vector of covariates (e.g. SST, air temperature), which affect the states; $\mathbf{C}_t$ is an $m \times p$ matrix of coefficients relating the effects of $\mathbf{c}_t$ to the $m \times 1$ state vector $\mathbf{x}_t$; $\mathbf{Q}_t$ is set so that the diagonal elements can be unequal and $\mathbf{x}_{t=0}$ from observed snail counts at $t = 1$.

The state variable model using the best-fitting subsets of covariates estimated positive autoregressive coefficients for the previous year's counts that were significantly different from 0 and from 1 for the PD small snails at both sites in July and for the DD small snails at NP only for both seasons (Table 1).

Table 1 shows that the ΔAICc values for the covariate subset that best fit the state variable model (Eq. 1) for the 4 life history by season combinations were 8.1 to 21.5 units smaller, indicating a better fit, than those for the same covariate subset fit to the multivariate linear regression model (MARSS model 13.3a in Table S3). Despite the poorer model fit without the autoregressive term, the 'slope' coefficients estimated by the multivariate linear regression model for the PD species in July at each site were identical in sign and very similar in magnitude (i.e. H_2: PP = −0.376, NP = −0.239; H_3: PP = 0.502, NP = 0.518; H_4: PP = 0.482, NP = 0.602 in Output S1 in Supplement 2 at www.int-res.com/articles/suppl/m753p085_supp2.pdf) to those estimated by the state variable model (Column 2 of Table 1).

Table 1 also shows that the subset of covariates that best fit the small snail count anomalies differed more between the 2 life history types (PD and DD) than between the July and December snail count surveys. Two covariates, SST_Feb and SST_Aug, were in the best covariate subset for the small PD snails for both July and December. Two different covariates, SSTbuoy_Feb and Salinity_Jul, were in the best covariate subset for small DD snails in July and in December. The *a priori* covariate SST_Feb was highly positively correlated with SSTbuoy_Feb (Pearson correlation r = 0.734, $p < 0.001$, N = 28). Nevertheless, the slope coefficients for these 2 similar SST covariates differed in sign for the PD and DD snails. SST_Feb had a positive 'slope' for the PD species which was significantly different from zero at both sites and seasons (Table 1). By contrast, the covariate SSTbuoy_Feb had a significant negative slope for the DD species at PP in July and for both sites in December.

Other members of the best covariate set differed between the PD and DD life history types. The *a priori* covariate SST_August, which, unlike SST_July, was uncorrelated with SST_Feb (Pearson correlation r = 0.191, $p < 0.313$, N = 30), had a significant positive 'slope' for the PD species for both sites in July and at NP in December (Table 1). The *a priori* covariate lined shore crab abundance 'PACHY-Jul' had a significant

Table 1. 'Slope' coefficients (lower, upper 95% confidence limits, CL) for the best-fitting subset of covariates to the best multivariate autoregressive state space (MARSS) state variable model (Eq. 1; Table S3) for the log10 count anomalies for small snails of each life history type (PD: planktonic developing from floating egg capsule, DD: direct developing from egg mass) by season (July, December) combination. Each set of covariates was fit simultaneously to the 2 study sites, Prasiola Point (PP) and Nudibranch Point (NP), but were fit separately for each season for PD (Table S6) and for DD (Table S7). Abbreviations: AICc: Akaike's information criterion corrected for small sample size for the subset of covariates listed in the first row; ΔAICc: difference in AICc between 2 models; CB: Cape Beale Lighthouse; LP: La Perouse buoy; max: maximum; min: minimum; NA: not applicable to this group because season does not match; PACHY: counts of the lined shore crab *Pachygrapsus crassipes*; sm: small size-class of snails with shell length between 1.5 and 3.4 mm; snails: *Littorina* spp.; SST: sea surface temperature; SSTbuoy: sea surface temperature from La Perouse moored buoy; sub: *L. subrotundata*; sc: *L. scutulata* sensu lato, which represents *L. scutulata* sensu stricto and *L. plena* combined counts; T: temperature. **Bold** values are defined separately in the footnotes

Covariates in model (or autoregressive terms)	July species		December species	
	PD smsc	DD smsub	PD smsc	DD smsub site
Covariates in best subset	SST_Feb, SST_Aug, PACHY_Jul	SSTbuoy_Feb, Salinity_Jul	SST_Feb, SST_Aug	SSTbuoy_Feb, Salinity_Jul, CB_meanmax_air_Jul
Model rank and (AICc)[a]	#1 (82.4)	#1 (124.9)	#1 (110.8)	#1 (140.0)
ΔAICc multivariate[b] linear regression: same covariates	(103.9) Δ = +21.5	(138.8) Δ = +13.9	(119.6) Δ = +8.8	(148.1) Δ = +8.1
H_2: temporarily invading lined shore crab counts[c] PACHY_Jul	PP **−0.332 (−0.537, −0.127)**[i] NP **−0.219 (−0.425, −0.0135)**[i]	[j]	[j]	[j]
H_3: warm seawater (SST) at survey time[d]: SST_Aug	PP **0.359 (0.0938 0.625)**[i] NP **0.481 (0.221, 0.740)**[i]	[j]	PP 0.290 (−0.0155, 0.595) NP **0.471 (0.186, 0.755)**[i]	[j]
H_4: warm seawater in previous February[e]: SST_Feb (for smsc) or SSTbuoy_Feb (for smsub)	PP **0.356 (0.140, 0.572)**[i] NP **0.518 (0.305, 0.731)**[i]	PP **−0.387 (−0.703, −0.0700)**[i] NP −0.142 (−0.472, 0.188)	PP **0.550 (0.294, 0.806)**[i] NP **0.525 (0.238, 0.811)**[i]	PP **−0.484 (−0.804, −0.165)**[i] NP **−0.3895 (−0.709, −0.0702)**[i]
July air temperatures[f]: CB_meanmax_air_Jul	[j]	[j]	[j]	PP −0.245 (−0.560, 0.0707) NP 0.194 (−0.134, 0.521)
Surface salinity from : satellite in July[g] SAL_JUL	[j]	**PP 0.0108 (−0.354, 0.375) NP 0.401 (0.0620, 0.739)**[i]	[j]	**PP 0.0407 (−0.304, 0.386) NP 0.161 (−0.159, 0.482)**
Autoregressive coefficients[h]: Density dependence between years for a particular season	PP **0.321 (0.109, 0.532)**[k] NP **0.216 (0.0173, 0.415)**[k]	PP 0.236 (−0.0821, 0.555) NP **0.331 (0.0145, 0.648)**[k]	PP −0.116 (−0.364, 0.131) NP −0.0199 (−0.290, 0.251)	PP 0.155 (−0.188, 0.497) NP **0.371 (0.0612, 0.682)**[k]

[a]Rank (by column within season × life history) of this model with this best subset of covariates with respect to AICc (smaller values indicate better fit). The best-fitting model presented here uses the state variable process-error-only autoregressive and mean-reverting model with the initial states determined by the data at time = 1 (model 13.4c in Table S3 in Supplement 1; Holmes et al. 2023)

[b]Decrease in fit (positive ΔAICc) of a multivariate linear regression (model 13.3.1 in Table S3; Supplement 2) using same covariates as independent variables and the log-transformed snail counts for that life history type at that season at both study sites as the 2 dependent variables

[c]Covariate temporarily invading predatory lined shore crab count anomalies during season snails sampled

[d]Covariate SST during August

[e]Covariate SST in previous February when Davidson northward current occurs

[f]Covariate Cape Beale mean maximum daily air temperature anomaly for the month of July was not one of the *a priori* hypotheses

[g]Covariate salinity was selected by stepwise multiple linear regression but was not one of the *a priori* hypotheses

[h]Autoregressive term showing whether the snail count at time *t* affects the snail count at *t*−1 for each life history type during a particular season

[i]**Bold** font indicates that the 95% confidence limits (Hessian method) for that covariate did not overlap zero

[j]Covariate not in subset of model with lowest AIC value

[k]**Bold** font indicates that the 95% confidence limits (Hessian method) for that autoregressive coefficient did not overlap zero or one

negative 'slope' only for the PD snail species in July at both sites (Table 1). The *a priori* covariate CB_meanmax_air_Jul was included in the best covariate subset for the DD snail species in December but its negative 'slope' was not significantly different from zero (Table 1). An interesting *a posteriori* covariate result was the significant positive 'slope' for Salinity_Jul only for the DD species at NP in July (Table 1).

Notably, covariate subsets that gave the lowest AICc values almost never included log count anomalies of small or large heterospecific snails until ΔAICc was much larger (>10) than the best covariate subset for that grouping (Tables S6 & S7). The only exception was small DD snails in December (smsubDec: ΔAICc = +1 in Table S7), but in that case, the 'slope' coefficients for the covariates (smscDec-PP or smscDec-NP) were not significantly different from zero.

The covariates 'SST_Feb', 'SST_Aug', and 'PACHY_Jul' (lined shore crab abundance) were chosen as the *a priori* hypothesis-relevant common subset of covariates of *a priori* covariates for the state-variable model (Eq. 1). This subset gave the lowest AICc values for the PD species (rank 1 within July and rank 2 within December) and moderately low AIC values for the DD species (rank 9 within July and rank 10 within December, respectively, Table S9). By contrast, covariate subsets that were fitted to both life history types simultaneously gave ΔAICc values that were at least twice as large (Table S8) than of those obtained when the same subsets were fitted to only one life history type (Table 2; Tables S6 & S7), supporting the single-species methodology used here. Table 2 shows the model results for all 4 life history by season groupings for the shared hypothesis-relevant

Table 2. 'Slope' coefficient (lower, upper 95% CL) for a common subset of covariates. Log_{10} small snail count anomalies for the 2 life history types were simultaneously fit to the same MARSS state variable model (Eq. 1) with a common subset of covariates (SST_Feb, SST_Aug, PACHY_Jul) to address Hypotheses 2 to 4. Models were fit separately for the July count anomalies and December count anomalies for each life history type (PD or DD). Abbreviations as in Table 1. **Bold** values are defined separately in the footnotes

Covariates in model (or autoregressive terms)	July species		December species	
	PD smsc	DD smsub	PD smsc	DD smsub site
Model rank and (AICc)[a]	#1 (82.4)	#9 (135.8)	#2 (111.5)	#10 (152.5)
H_2: Temporarily invading lined shore crab counts[b] PACHY_Jul	PP **−0.332** **(−0.537, −0.127)**[f] NP **−0.219** **(−0.425, −0.0135)**[f]	PP −0.266 (−0.589, 0.0562) NP −0.133 (−0.459, 0.194)	PP 0.206 (−0.0385, 0.450) NP −0.0418 (−0.286, 0.202)	PP 0.0396 (−0.311, 0.390) NP 0.0881 (−0.257, 0.433)
H_3: Warm seawater (SST) at survey time[c]: SST_Aug	PP **0.359** **(0.0938 0.625)**[f] NP **0.481** **(0.221, 0.740)**[f]	PP −0.0433 (−0.467, 0.381) NP −0.138 (−0.622, 0.346)	PP 0.217 (−0.0922, 0.527) NP **0.485** **(0.195, 0.776)**[f]	PP −0.16824 (−0.6074, 0.2709) NP −0.00556 (−0.419, 0.430)
H_4: Warm seawater in previous February[d]: SST_Feb	PP **0.356** **(0.140, 0.572)**[f] NP **0.518** **(0.305, 0.731)**[f]	PP **−0.326** **(−0.634, −0.0170)**[f] NP −0.1107 (−0.4257, 0.204)	PP **0.546** **(0.297, 0.795)**[f] NP **0.524** **(0.246, 0.802)**[f]	PP **−0.378** **(−0.715, −0.0408)**[f] NP −0.244 (−0.580, 0.0933)
Autoregressive coefficients[e]: Density dependence between years for a particular season	PP **0.321** **(0.109, 0.532)**[g] NP **0.216** **(0.0173, 0.415)**[g]	PP 0.222 (−0.0825, 0.526) NP 0.403 (−0.00107, 0.807)	PP −0.102 (−0.338, 0.135) NP −0.0190 (−0.278, 0.240)	PP 0.240 (−0.105, 0.584) NP **0.357** **(0.0190, 0.695)**[g]

[a]Rank (by column within season × life history) of this model with this shared subset of covariates relative to the same model with other subsets of covariates with respect to AICc (smaller values indicate better fit). The best-fitting model presented here uses the state variable process-error-only autoregressive and mean-reverting model with the initial states determined by the data at time = 1 Model 13.4c in Table S3 in Supplement 1 (Holmes et al. 2023).

[b]Covariate temporarily invading predatory lined shore crab count anomalies during snail sampling season

[c]Covariate SST during August

[d]Covariate SST in previous February when Davidson poleward current occurs

[e]Autoregressive term showing whether the density at time *t* affects the density at *t*−1

[f]**Bold** font indicates the covariate slope coefficient was significant because its 95% confidence limits (Hessian method) did not overlap zero

[g]**Bold** font indicates the autoregressive slope coefficient was significant because its 95% confidence limits (Hessian method) did not overlap zero or one

common subset of covariates. The covariate SST in February had significant positive 'slope' coefficients for both season and sites for all PD and significant negative slope coefficients for all DD except for NP in December (Table 2). The covariate SST in August had positive 'slope' coefficients that were significant for PD at both sites in July and at NP in December (Table 2). The covariate 'PACHY_Jul' had a negative 'slope' that was significantly different from zero only for PD in July (Table 2). Finally, the autoregressive component that used only the previous year's counts showed positive coefficients that were significantly different from 0.0 and from 1.0 for the PD small snails at both sites in July and for the DD small snails only at NP in December (Table 2). The autoregressive coefficients were no longer significant for the DD snails at NP in July, which may reflect poorer fit to the 'State' variable model for the DD snails with this common subset of covariates.

4. DISCUSSION

4.1. Life history effects on recruitment

The best-fitting MARSS model class to my snail count anomalies was a state variable process-error-only, mean-reverting model with initial values of x at time 0 determined by my 28 yr time series data set. The state variable only model class fit better than the 2 model classes which also contained a second equation that modelled errors in the count observations (Table S3 & Supplement 2). This suggests that my count 'observations' of the juvenile snails of each life history type were unbiased estimates of their true state values.

The state variable model also fit better than a multivariate linear regression model that lacks the autoregressive term of the state variable model which related the current juvenile snail counts of each life history type to their juvenile counts during the same season of the previous year. For the MARSS models of log-transformed counts, an autoregressive coefficient of one corresponds to density independence, but as the coefficient approaches zero, density dependence increases (Ives et al. 2003). The autoregressive component of the State variable model estimated positive coefficients of 0.2–0.4 with 95% confidence limits that did not overlap 0 or 1.0, indicating moderate density dependence for the PD at both sites in July only and for the DD at NP only during both seasons (Table 1). The autoregressive coefficients were similar in sign and magnitude when a hypothesis-relevant common subset of covariates (Table 2) that fit the PD snails better than the DD snails was used. The moderate positive autoregressive coefficients for the small PD snails were surprising, but could arise from limited abiotic or biotic refuges available to newly settled PD snail postlarvae (Boulding & Harper 2011, Silva et al. 2015). The very low juvenile PD counts, which are significantly higher during very strong El Niño years, suggest that larval supply is limited solely by covariates correlated with El Niño events, thus supporting the larval supply hypothesis (Gaines & Roughgarden 1985, Connolly & Roughgarden 1999, Lundquist et al. 2000).

The best subset of covariates for the best-fitting state variable model class showed no support for H_1 (interspecific competition) or H_2 (differential predation by an invading crab). This model class showed some support for H_3 (warm August temperature) for the PD species only and strong support for H_4 (El Niño effects on SST and poleward currents the previous February) (Table 3). H_3, which postulates that the PD species show increased growth and survival when the summer SSTs are warmer but that the DD species does not, was supported by the significant positive 'slope' coefficients between the August SST covariate and the July count anomalies at both sites and by the December count anomalies at PP for the PD species (Tables 1 & 2). However, the coefficients for the August SST covariate were not significantly different from zero for the DD snail species (Table 2).

H_4 postulates that large numbers of PD *Littorina scutulata* sensu lato larvae were transported north in the warmer and stronger winter Davidson current that forms during very strong El Niño events, which has been shown here (Fig. 3B) and previously for the non-indigenous lined shore crab (Boulding et al. 2020, Behrens Yamada et al. 2022). It is more difficult to show that the increased intertidal recruitment of PD *L. scutulata* s. l. is a result of transport of its larvae because it is an indigenous species at both study sites (PP and NP). It would also be more difficult to count competent planktonic snail larvae than it is to count crab larvae (Shanks & Brink 2005, Rasmuson & Shanks 2020) because the snail larvae are smaller (400 µm versus 2000–3000 µm) and because they do not cling to string mops mounted under night lights as crab megalopae do (but see Strathmann 2023). The July and December log10 count anomalies for small snails of the PD species were largest only after the very strong El Niño events. These very strong El Niño events were correlated with anomalously warm SST the previous February. Indeed, the covariate February SST had a significant positive slope for the PD species during both seasons

Table 3. Conclusions from MARSS state covariate models for the July–August (July) and December–January (December) quadrat counts of recent recruits (1.5–3.4 mm shell length) of the *Littorina* on the 2 rocky intertidal shores (PP: Prasiola Point and NP: Nudibranch Point). In the model (left) column, the first line is the environmental covariate. The middle column has the mechanism by which the covariate is postulated to affect the snail count anomaly. Some environmental covariates were postulated to positively affect the snails with planktonic egg and planktotrophic larval stages (PD) and negatively affect the snails with crawl-away juveniles that developed directly from an attached egg mass (DD). sm: small size-class of snails with shell length between 1.5 and 3.4 mm; sc: *L. scutulata* sensu lato, which represents *L. scutulata* sensu stricto and *L. plena* combined counts; sub: *L. subrotundata*; PACHY: counts of the lined shore crab *Pachygrapsus crassipes*; SST: sea surface temperature

	Covariates	Postulated effect during very strong El Niño events	MARSS model coefficient support?
H_1	Yearly count anomalies for small snails (new recruits) with different developmental mode vary inversely. PD smsc vs. DD smsub	Interspecific competition between DD and PD small snails for topographical refuges or food	Reject H_1. Spearman correlations between DD and PD small *Littorina* species raw counts from the same quadrats were significantly positive. Best-fitting MARSS covariate subsets almost never included densities of heterospecific snails (Tables S6, S7, S9 in Supplement 1)
H_2	Temporary invading lined shore crab *Pachygrapsus crassipes* counts from summer. PACHY_Jul	Higher predation of thin-shelled DD snail species than of thicker-shelled PD species by lined shore crab	No support for covariate slope being more negative for DD snail anomalies than for PD snail anomalies. Support for predatory lined shore crab covariate reducing July PD count anomalies, covariate slope is significantly negative for PD only (Tables 1 & 2).
H_3	August SST	Warm summer SST and air temperature anomalies increased recruitment of the PD species and reduced recruitment of the DD species	Support for PD only – in July at both PP and NP and also in December at NP only with significant positive 'slopes' for Aug SST for their best covariate subset model (Table 1) and in the shared covariate subset model (Table 2).
H_4	Previous February SST (or February buoy SST)	Warm SST anomalies in the previous February suggest that augmented northward transport of snail larvae in warm Davidson current, and perhaps also cross-shelf transport onshore, increases the recruitment of the PD species only	Supported (Table 2). PD have significant positive slope coefficients. All DD have significant negative slope coefficients except NP in December (Table 1) and NP in July (Table 2).

at both sites, whereas the slopes for the DD species were significantly negative at both sites in July and at PP in December (Table 2; Table S5). Even when the best-fitting covariate subset for each life history by season grouping was used (Table 1), the covariate SSTbuoy_Feb, which was highly correlated with the February Hadley SST anomaly (Fig. S8, Table S5), had a significant negative slope for the DD species in July and at both sites in December (Table 1). The Hadley satellite SST, the LP buoy SST, and the ONC subsurface observatories showed the anomalously warmer minimum winter SST in Barkley Sound (Figs. S8–S10), all of which support H_4. Warmer minimum temperatures during the February preceding severe El Niño events will increase PD larval growth or survival by reducing the developmental time of *L. scutulata* s. l. (Buckland-Nicks et al. 1973), thereby reducing the number of days its egg capsule and larvae must spend in the plankton, where mortality is higher (Strathmann 2023). The new recruits of the PD species synchronously became more abundant at both study sites after the very strong 1997–1998 and 2015–2016 El Niño events, and to a lesser extent in 1994 after the strong 1992 El Niño event, which also supports H_4. This suggests that their larval stages were positively affected by the warmer minimum SST temperatures and supports the supply-side ecology hypothesis that PD *Littorina* distribution and abundance at the 2 study sites was a function of the supply of competent larvae (Gaines & Roughgarden 1985, Connolly & Roughgarden 1999, Goode et al. 2019).

4.2. H_1: Interspecific competition

In the time series plots, the negative correlation between the count anomaly of the DD species and

that of the PD species initially suggested that interspecific competition for food or biogenic refuges amongst barnacles might be occurring, as is documented for other *Littorina* species (Behrens Yamada & Mansour 1987). However, I found significant and positive Spearman rank correlations between counts of PD and DD *Littorina* species from the same quadrat except for December at PP, when the correlation was close to zero.

Further, in the only case (small DD snails in December) when a subset of covariates in a MARSS model included the count anomalies for small (or large) heterospecific snails of the other life history type had a ΔAICc close to that (+1) of the best covariate subset, the 'slope' coefficients obtained did not significantly differ from zero. This allowed rejection of the hypothesis that interspecific competition from the increased abundance of PD *Littorina* species was responsible for the decline of the normally abundant DD *L. subrotundata* during the second major El Niño event. A recent review suggests that negative co-occurrence is poor evidence for interspecific competition (Brazeau & Schamp 2019).

4.3. H_2: Selective predation of DD snails by an invading shore crab

Zoeae and megalopae of the non-indigenous lined shore crab *Pachygrapsus crassipes* from south of Coos Bay, OR (Behrens Yamada et al. 2022), were transported north to the west coast of Vancouver Island in the 1987–1988 and in the 2015–2016 El Niño-augmented winter Davidson current (Boulding et al. 2020). During the 2 very strong El Niño events (1997–1998 and 2015–2016) and for several years afterwards, lined shore crabs were found at both study sites (Cassone & Boulding 2006, Boulding et al. 2020). This was of interest because the historical northern range limit of *P. crassipes* is near Coos Bay, OR, which is 600 km south of Bamfield and coincides with the southern range limit of *L. sitkana* (Behrens Yamada 1977, Reid 1990). The thin-shelled DD species *L. subrotundata* is even more vulnerable to purple shore crab *Hemigrapsus nudus* predation than is *L. sitkana* (Boulding & Van Alstyne 1993, Boulding et al. 1999, 2007, Pakes & Boulding 2010), whereas the 2 thick-shelled PD *Littorina* species are more resistant to lined crab predation than is *L. sitkana* (Boulding et al. 2020). Although the covariate 'lined shore crab counts' had negative slopes for all 4 groupings, the slopes were significantly negative only for PD snails in July. Therefore, the *a priori* hypothesis of selectively high predation on the thin-shelled DD relative to the thick-shelled PD species was not supported. Instead, what may be causing the only significant negative slope is larval lined shore crab predation on the *Littorina* egg capsules (Strathmann 2023) or post-larvae (Gosselin & Chia 1995) of the PD species.

4.4. H_3: Differential responses to warm seawater

The strong El Niño of 2015–2016 is thought to be unusual in that it was immediately preceded by the Northeastern Pacific 'Blob' anomaly (Tseng et al. 2017). The Blob was a highly stratified surface pool of seawater with a deviation of 2.5°C above normal conditions that formed near the Gulf of Alaska in late Fall 2013 and then expanded down to Vancouver Island and then to Baja California in 2014 until it was dissipated by the La Niña of late winter 2016 (Jacox et al. 2016, Tseng et al. 2017). The Blob warm water anomaly resulted in several pelagic subtropical fish and invertebrate species extending their range northward (Bond et al. 2015, Sanford et al. 2019). The Blob increased the air and land temperatures downwind, which caused a heat wave. The negative surface wind anomaly, positive air temperature anomaly, and low summer 2016 rainfall produced by the 2015–2016 El Niño may have been responsible for the near disappearance of small juvenile snails and large adults of the direct-developing *L. subrotundata* from my quadrats since their positive anomaly in 2013. A search outside my quadrats in 2016 verified that a few DD adult *L. subrotundata* were present inside shaded deep cracks and on seaward-facing vertical cliffs. High mortality during the Northeastern Pacific Blob was also observed for the middle intertidal acorn barnacle *Semibalanus cariosus*; barnacles attached to substrates that received more direct solar irradiance had higher death rates (Hesketh & Harley 2023). The current study suggests a new hypothesis, that climate change is significantly decreasing the abundance of large DD *L. subrotundata* (Figs. S6D & S7D), particularly at the NP site. The effects of climate change are not entirely explained by latitude. For example, the rocky intertidal fauna in Shetland showed an increase in warm-affinity species that was correlated with local warming from 1980 to 2018, whereas fauna in the southwest British Isles showed an increase in cold-affinity species and a decrease in warm-affinity species, correlated with ocean cooling between 2002 and 2018 (Burrows et al. 2020).

4.5. H_4: Larval transport and planktotrophic snail count anomalies

Very strong El Niño events are recognisable because of an increase in sea height caused by the propagation of coastal Kelvin waves that El Niño creates (Allen & Hsieh 1997). Forecasts of sea surface height (SSH) anomalies from a GLORYS oceanographic model were highly correlated with SSH anomalies measured by tide gauges during the very strong El Niño event between 1 January 2015 and 30 April 2016, as coastally trapped Kelvin waves were propagated along the continental shelf at 2.7 m s^{-1} (Amaya et al. 2022). Eight drifter buoys deployed off Newport, OR (44.658° N), during the downwelling period between 30 January and 2 February 1998, nearly all moved northward towards Vancouver Island at an average speed of 0.26 m s^{-1} because of an unusually strong northward Davidson current over the inner continental slope that had been augmented by the 1997–1998 El Niño (Austin & Barth 2002). Very strong El Niño events are also recognisable by the rapid increase in SST (Allen & Hsieh 1997). The transport of warm water poleward by coastal Kelvin waves along the continental shelf was supported by the Folger Deep cable observatory at 100 m, showing a warm seawater anomaly in 2015–2016 that was not observed in 2014. By contrast, the Folger Pinnacle cable observatory at 25 m showed a warm anomaly in 2014 that began when the Northeast Pacific Blob was still present.

Previous larval and oceanographic studies support the hypothesis that during very strong El Niño events, planktotrophic eggs and larvae of intertidal species are transported northward in a warmer and stronger Davidson current, which flows northward from California to the southern west coast of Vancouver Island every winter (Reid & Schwartzlose 1962, Mackas et al. 2001). El Niño effects on SST decrease faster than those on sea level height poleward of Southern California (Lluch-Cota et al. 2001), which may explain why larval transport to Vancouver Island from California only happens during very strong El Niño events. During the very strong 1983 El Niño, southern marine fauna were reported off Washington State (Pearcy & Schoener 1987) and also off the west coast of Canada (Mysak 1986). Zoeae and megalopae belonging to non-indigenous European green shore crabs were transported north during the winter 2016 very strong El Niño (Behrens Yamada & Kosro 2010, Behrens Yamada et al. 2015, 2022).

Once any transported *L. scutulata* s. l. larvae arrived offshore, the reduced summer upwelling off the central west coast of Vancouver Island that occurs during El Niño events may have facilitated their cross-shelf transport onshore towards the intertidal zone (Connolly & Roughgarden 1999, Lundquist et al. 2000, Navarrete et al. 2002, Poulin et al. 2002, Narváez et al. 2006, Broitman et al. 2008, Dudas et al. 2009). Regardless of the source of the larvae, recruitment of offshore planktonic larvae back to the intertidal zone requires crossing the fall–winter poleward flowing buoyancy-driven current off Vancouver Island (Hickey et al. 1991, Behrens Yamada et al. 2022). Summer changes in wind direction reduce the strength of the Vancouver Island Buoyancy current (Foreman et al. 2024). Current meters deployed at 50 m depth off the west coast of Vancouver Island show that the flow along Vancouver Island in January and February between 1979 and 1982 is towards the northwest at 8 cm s^{-1}, parallel to shore and reaches 30–40 cm s^{-1} at 15 km from shore; off Barkley Sound, the currents are weak during the spring transition in March and on average turn southward in April (Freeland et al. 1984). In addition, summer wind reversals off Vancouver Island during the 2 strong El Niño events reduced upwelling and increased downwelling, which may have facilitated the onshore transport of competent *Littorina* larvae. This is supported by Figs. 2 & 3, which show that *L. scutulata* s. s. and *L. plena* only showed a high recruitment rate during strong El Niño events. This is also supported by increased barnacle recruitment at a coastal site in Oregon that experienced more frequent reversals of the predominantly equatorward currents because of the 1998 El Niño event; barnacle recruitment increased with increasing temperature and when the cross-shelf flow was onshore (Dudas et al. 2009).

H_4 postulates a high-speed poleward larval transport mechanism during very strong El Niño events, which can explain the temporal fluctuations in allele frequencies previously documented (Lee & Boulding 2009) for populations of *Littorina* species with planktotrophic larvae. There is indirect evidence from population genetic studies for non-local recruitment of *L. plena* and *L. scutulata* to Barkley Sound populations, including to PP and NP. Temporal fluctuations in mitochondrial haplotype frequencies and nuclear allele frequencies (Lee & Boulding 2009) of *Littorina* PD larvae have been attributed to sweepstakes reproductive success of a cohort of females from along the geographical range of these species (Hedgecock 1994, Hedgecock et al. 2007, Hedgecock & Pudovkin 2011).

4.6. Summary

Two species of PD and 2 species of DD *Littorina* were counted semi-annually at 2 independent rocky intertidal study sites between 1994 and 2021. The intertidal recruitment of the PD species was positively correlated with very strong El Niño events, whereas the recruitment of the wave-exposed DD species was negatively correlated. Four *a priori* working hypotheses that explained the inverse recruitment log10 count anomalies of PD and DD *Littorina* spp. were evaluated using separate MARSS state variable only models for each life history type and season and a hypothesis-relevant subset of covariates. Spearman rank correlation analysis by site and season found significant positive interspecific correlations for snails from the same quadrats, which allowed rejection of the hypothesis that the inverse recruitment anomalies of PD and DD *Littorina* spp. were from interspecific competition. The MARSS analysis rejected the hypothesis that they resulted from the differential vulnerability of the thin-shelled DD species to predation by the invading lined shore crab. The MARSS analysis partially supported the hypothesis that there was a differential response to warmer seawater during August in that the slope coefficients were significantly positive for the PD at both sites in July and at PP in December. Most notably, the MARSS analysis estimated significant positive 'slope' coefficients for the PD species in both seasons and at both sites and significant negative 'slope' coefficients for the DD species in July at PP and at both sites in December. This provided strong support for the hypothesis that very strong El Niño events that resulted in a higher minimum SST the previous February increased PD recruitment because the winter Davidson current was warmer and was flowing northward at a higher speed. This suggests that the positive recruitment anomalies of PD *Littorina* were related to very strong El Niño events whereby their eggs and larvae are transported in warm winter seawater poleward, and likely also transported across the shelf towards shore.

Acknowledgements. I thank E. N. Hay, E. Merlot, T. Prizing, A. Riley, K. Riley, P. I. Stuart, and many other short-term technicians and volunteers for assistance with collecting and sorting of gastropod samples. I also thank E. Sanford and anonymous reviewers for improving the final paper, T. Hay and A. Tie Ten Quee for proofreading, and X. Ge for creating the R script for Fig. 1. Bamfield Marine Science Centre provided me with accommodation, motorboats, and laboratory support, and Strathcona Park Lodge Outdoor Education Centre lent me vehicles and kayaks. The Huu-ay-aht First Nation permitted access to my study sites at Second Beach. Financial support was provided by continuous Discovery Grants from the Natural Sciences and Engineering Research Council of Canada (RGPIN-2020-05150) and an Ontario Premier's Research Excellence Award.

LITERATURE CITED

Akaike H (1978) On the likelihood of a time series model. Statistician 27:217–235

Allen SE, Hsieh WW (1997) How does the El Niño-generated coastal current propagate past the Mendocino escarpment? J Geophys Res 102:24977–24985

Amaya DJ, Jacox MG, Dias J, Alexander MA, Karnauskas KB, Scott JD, Gehne M (2022) Subseasonal-to-seasonal forecast skill in the California Current system and its connection to coastal Kelvin waves. J Geophys Res Oceans 127:e2021JC017892

Anderson DR (2008) Model based inference in the life sciences: a primer on evidence. Springer, New York, NY

Anderson DR, Burnham KP (2002) Avoiding pitfalls when using information-theoretic methods. J Wildl Manag 66: 912–918

Auger-Méthé M, Newman K, Cole D, Empacher F and others (2021) A guide to state–space modeling of ecological time series. Ecol Monogr 91:e01470

Austin JA, Barth JA (2002) Drifter behavior on the Oregon-Washington Shelf during downwelling-favorable winds. J Phys Oceanogr 32:3132–3144

Behrens Yamada S (1977) Geographic range limitation of the intertidal gastropods *Littorina sitkana* and *L. planaxis.* Mar Biol 39:61–65

Behrens Yamada S (1989) Are direct developers more locally adapted than planktonic developers? Mar Biol 103: 403–411

Behrens Yamada S, Kosro PM (2010) Linking ocean conditions to year class strength of the invasive European green crab, *Carcinus maenas.* Biol Invasions 12:1791–1804

Behrens Yamada S, Mansour RA (1987) Growth inhibition of native *Littorina saxatilis* (Olivi) by introduced *L. littorea* (L.). J Exp Mar Biol Ecol 105:187–196

Behrens Yamada S, Peterson WW, Kosro PM (2015) Biological and physical ocean indicators predict the success of an invasive crab, *Carcinus maenas*, in the northern California Current. Mar Ecol Prog Ser 537:175–189

Behrens Yamada S, Fisher JL, Kosro PM (2021) Relationship between ocean ecosystem indicators and year class strength of the invasive European green crab (*Carcinus maenas*). Prog Oceanogr 196:102618

Behrens Yamada S, Shanks AL, Thomson RE (2022) Can the timing and duration of planktonic larval development contribute to invasion success? A case study comparing range expansion in the European green crab, *Carcinus maenas*, and the native lined shore crab, *Pachygrapsus crassipes*, in the northeast Pacific. Biol Invasions 24: 2917–2932

Bond NA, Cronin MF, Freeland H, Mantua N (2015) Causes and impacts of the 2014 warm anomaly in the NE Pacific. Geophys Res Lett 42:3414–3420

Boulding EG, Harper FM (2011) Increasing precision in randomised field experiments: barnacle microtopography as a predictor of *Littorina* abundance. Hydrobiologia 378: 105–114

Boulding EG, Van Alstyne KL (1993) Mechanisms of differential survival and growth of two species of *Littorina* on wave-exposed and on protected shores. J Exp Mar Biol Ecol 169:139–166

Boulding EG, Buckland-Nicks J, Van Alstyne Katherine L (1993) Morphological and allozyme variation in *Littorina sitkana* and related *Littorina* species from the northeastern Pacific. Veliger 36:43–68

Boulding EG, Holst M, Pilon V (1999) Changes in selection on gastropod shell size and thickness with wave-exposure on northeastern Pacific shores. J Exp Mar Biol Ecol 232:217–239

Boulding EG, Hay T, Holst M, Kamel S, Pakes D, Tie AD (2007) Modelling the genetics and demography of step cline formation: gastropod populations preyed on by experimentally introduced crabs. J Evol Biol 20: 1976–1987

Boulding EG, Rivas MJ, González-Lavín N, Rolán-Alvarez E, Galindo J (2017) Size selection by a gape-limited predator of a marine snail: insights into magic traits for speciation. Ecol Evol 7:674–688

Boulding EG, Behrens Yamada S, Schooler SS, Shanks AL (2020) Periodic invasions during El Niño events by the predatory lined shore crab (*Pachygrapsus crassipes*): forecasted effects of its establishment on direct-developing indigenous prey species (*Littorina* spp.). Can J Zool 98: 787–797

Brazeau HA, Schamp BS (2019) Examining the link between competition and negative co-occurrence patterns. Oikos 128:1358–1366

Broitman BR, Blanchette CA, Menge A, Lubchenco J and others (2008) Spatial and temporal patterns of invertebrate recruitment along the west coast of the United States. Ecol Monogr 78:403–421

Buckland-Nicks J, Chia FS, Behrens S (1973) Oviposition and development of two intertidal snails, *Littorina sitkana* and *Littorina scutulata.* Can J Zool 51:359–365

Burrows MT, Hawkins SJ, Moore JJ, Adams L, Sugden H, Firth L, Mieszkowska N (2020) Global-scale species distributions predict temperature-related changes in species composition of rocky shore communities in Britain. Glob Change Biol 26:2093–2105

Cahill AE, Aiello-Lammens ME, Fisher-Reid MC, Hua X and others (2013) How does climate change cause extinction? Proc R Soc B 280:20121890

Cahill AE, Aiello-Lammens ME, Fisher-Reid MC, Hua X and others (2014) Causes of warm-edge range limits: systematic review, proximate factors and implications for climate change. J Biogeogr 41:429–442

Cassone BJ, Boulding EG (2006) Genetic structure and phylogeography of the lined shore crab, *Pachygrapsus crassipes*, along the Northeastern and Western Pacific coasts. Mar Biol 149:213–226

Chow V (1987) Patterns of growth and energy allocation in northern California populations of *Littorina* (Gastropoda: Prosobranchia). J Exp Mar Biol Ecol 110:69–89

Chow V (1989) Intraspecific competition in a fluctuating population of *Littorina plena* Gould (Gastropoda: Prosobranchia). J Exp Mar Biol Ecol 130:147–165

Connell JH (1961) Effects of competition, predation by *Thais lapillus*, and other factors on natural populations of the barnacle *Balanus balanoides.* Ecol Monogr 31:61–104

Connolly SR, Roughgarden J (1999) Increased recruitment of northeast Pacific barnacles during the 1997 El Niño. Limnol Oceanogr 44:466–469

Dudas SE, Grantham BA, Kirincich AR, Menge BA, Lubchenco J, Barth JA (2009) Current reversals as determinants of intertidal recruitment on the central Oregon coast. ICES J Mar Sci 66:396–407

Farrell TM, Bracher D, Roughgarden J (1991) Cross-shelf transport causes recruitment to intertidal populations in central California. Limnol Oceanogr 36:279–288

Foreman MGG, Chandler PC, Bianucci L, Wan D and others (2024) A circulation model for inlets along the central west coast of Vancouver Island. Atmos-Ocean 62:58–89

Freeland HJ, Crawford WR, Thomson RE (1984) Currents along the Pacific coast of Canada. Atmos-Ocean 22: 151–172

Gaines S, Roughgarden J (1985) Larval settlement rate: a leading determinant of structure in an ecological community of the marine intertidal zone. Proc Natl Acad Sci USA 82:3707–3711

Goode AG, Brady DC, Steneck RS, Wahle RA (2019) The brighter side of climate change: how local oceanography amplified a lobster boom in the Gulf of Maine. Glob Change Biol 25:3906–3917

Gosselin LA, Chia FS (1995) Distribution and dispersal of early juvenile snails: effectiveness of intertidal microhabitats as refuges and food sources. Mar Ecol Prog Ser 128: 213–223

Hampton SE, Holmes EE, Scheef LP, Scheuerell MD, Katz SL, Pendleton DE, Ward EJ (2013) Quantifying effects of abiotic and biotic drivers on community dynamics with multivariate autoregressive (MAR) models. Ecology 94: 2663–2669

Hedgecock D (1994) Does variance in reproductive success limit effective population sizes of marine organisms? In: Beaumont A (ed) Genetics and evolution of aquatic organisms. Springer Science & Business Media, Dordrecht, Netherlands, p 122–132

Hedgecock D, Pudovkin AI (2011) Sweepstakes reproductive success in highly fecund marine fish and shellfish: a review and commentary. Bull Mar Sci 87:971–1002

Hedgecock D, Launey S, Pudovkin I, Naciri Y, Lapègue S, Bonhomme F (2007) Small effective number of parents (N_b) inferred for a naturally spawned cohort of juvenile European flat oysters *Ostrea edulis*. Mar Biol 150:1173–1182

Hesketh AV, Harley CDG (2023) Extreme heatwave drives topography-dependent patterns of mortality in a bed-forming intertidal barnacle, with implications for associated community structure. Glob Change Biol 29:165–178

Hickey BM, Thomson RE, Yih H, LeBlond PH (1991) Velocity and temperature fluctuations in a buoyancy-driven current off Vancouver Island. J Geophys Res 96: 10507–10538

Hohenlohe PA (2002) Life history of *Littorina scutulata* and *L. plena*, sibling gastropod species with planktotrophic larvae. Invertebr Biol 121:25–37

Holmes EE, Ward EJ, Wills K (2012) MARSS: multivariate autoregressive state-space models for analyzing time-series data. R J 4:11–19

Holmes EE, Smitha BR, Nimit K, Maity S, Checkley DM Jr, Wells ML, Trainer VL (2021) Improving landings forecasts using environmental covariates: a case study on the Indian oil sardine (*Sardinella longiceps*). Fish Oceanogr 30:623–642

Holmes EE, Holmes EE, Scheuerell MD, Ward EJ (2023) Analysis of multivariate time-series using the MARSS package version 3.11.7. https://atsa-es.r-universe.dev/MARSS/doc/UserGuide.pdf (accessed 29 Jan 2025)

Hughes RN, Roberts DJ (1981) Comparative demography of *Littorina rudis, L. nigrolineata* and *L. neritoides* on three contrasted shores in North Wales. J Anim Ecol 50: 251–268

Hull SL, Grahame JW, Mill PJ (1996) Morphological divergence and evidence for reproductive isolation in *Littorina saxatilis* (Olivi) in Northeast England. J Molluscan Stud 62:89–99

Huyer A, Smith RL (1985) The signature of El Niño off Oregon, 1982–1983. J Geophys Res Oceans 90:7133–7142

Huyer A, Smith RL, Fleischbein J (2002) The coastal ocean off Oregon and northern California during the 1997–8 El Niño. Prog Oceanogr 54:311–341

Ives AR, Dennis B, Cottingham KL, Carpenter SR (2003) Estimating community stability and ecological interactions from time-series data. Ecol Monogr 73:301–330

Jacox MG, Hazen EL, Zaba KD, Rudnick DL, Edwards CA, Moore AM, Bograd SJ (2016) Impacts of the 2015–2016 El Niño on the California Current System: early assessment and comparison to past events. Geophys Res Lett 43:7072–7080

Johannesson K, Johannesson B, Rolán-Alvarez E (1993) Morphological differentiation and genetic cohesiveness over a microenvironmental gradient in the marine snail *Littorina saxatilis*. Evolution 47:1770–1787

Kelly RP, Palumbi SR (2010) Genetic structure among 50 species of the northeastern Pacific rocky intertidal community. PLOS ONE 5:e8594

Kess T, Brachmann M, Boulding EG (2021) Putative chromosomal rearrangements are associated primarily with ecotype divergence rather than geographic separation in an intertidal, poorly dispersing snail. J Evol Biol 34:193–207

Kosro PM (2002) A poleward jet and an equatorward undercurrent observed off Oregon and northern California, during the 1997–98 El Niño. Prog Oceanogr 54:343–360

Kyle CJ, Boulding EG (2000) Comparative population genetic structure of marine gastropods (*Littorina* spp.) with and without pelagic larval dispersal. Mar Biol 137: 835–845

Lee HJ, Boulding EG (2009) Spatial and temporal population genetic structure of four northeastern Pacific littorinid gastropods: the effect of mode of larval development on variation at one mitochondrial and two nuclear DNA markers. Mol Ecol 18:2165–2184

Lee HJ, Boulding EG (2010) Latitudinal clines in body size, but not in thermal tolerance or heat-shock cognate 70 (*HSC70*), in the highly-dispersing intertidal gastropod *Littorina keenae* (Gastropoda: Littorinidae). Biol J Linn Soc 100:494–505

Little C, Trowbridge CD, Williams GA, Hui TY, Pilling GM, Morritt D, Stirling P (2021) Response of intertidal barnacles to air temperature: long-term monitoring and in-situ measurements. Estuar Coast Shelf Sci 256:107367

Lluch-Cota DB, Wooster WS, Hare SR (2001) Sea surface temperature variability in coastal areas of the northeastern Pacific related to the El Niño-Southern Oscillation and the Pacific Decadal Oscillation. Geophys Res Lett 28: 2029–2032

Lundquist CJ, Botsford LW, Morgan LE, Diehl JM, Lee T, Lockwood DR, Pearson EL (2000) Effects of El Niño and La Niña on local invertebrate settlement in Northern California. Calif Coop Ocean Fish Invest Rep 41:167–176

Mackas DL, Thomson RE, Galbraith M (2001) Changes in the zooplankton community of the British Columbia continental margin, 1985-1999, and their covariation with oceanographic conditions. Can J Fish Aquat Sci 58: 685–702

Mastro E, Chow V, Hedgecock D (1982) *Littorina scutulata* and *Littorina plena*: sibling species status of two prosobranch gastropod species confirmed by electrophoresis. Veliger 24:239–246

Menge BA, Cerny-Chipman EB, Johnson A, Sullivan J, Gravem S, Chan F (2016a) Correction: sea star wasting disease in the keystone predator *Pisaster ochraceus* in Oregon: insights into differential population impacts, recovery, predation rate, and temperature effects from long-term research. PLOS ONE 11:e0157302

Menge BA, Cerny-Chipman EB, Johnson A, Sullivan J, Gravem S, Chan F (2016b) Sea star wasting disease in the keystone predator *Pisaster ochraceus* in Oregon: insights into differential population impacts, recovery, predation rate, and temperature effects from long-term research. PLOS ONE 11:e0153994

Merlo EM, Milligan KA, Sheets NB, Neufeld CJ and others (2018) Range extension for the region of sympatry between the nudibranchs *Hermissenda opalescens* and *Hermissenda crassicornis* in the Northeastern Pacific. Facets 3:764–776

Meyer AD, Hastings A, Largier JL (2021) Larvae of coastal marine invertebrates enhance their settling success or benefits of planktonic development — but not both — through vertical swimming. Oikos 130:2260–2278

Mieszkowska N, Burrows MT, Hawkins SJ, Sugden H (2021) Impacts of pervasive climate change and extreme events on rocky intertidal communities: evidence from long-term data. Front Mar Sci 8:642764

Murray TE (1979) Evidence for an additional *Littorina* species and a summary of the reproductive biology of *Littorina* from California. Veliger 21:469–474

Mysak L (1986) El Niño, interannual variability and fisheries in the Northeast Pacific Ocean. Can J Fish Aquat Sci 43: 464–497

Narváez DA, Navarrete SA, Largier J, Vargas CA (2006) Onshore advection of warm water, larval invertebrate settlement, and relaxation of upwelling off central Chile. Mar Ecol Prog Ser 309:159–173

Navarrete SA, Broitman B, Wieters EA, Finke GR, Venegas RM, Sotomayor A (2002) Recruitment of intertidal invertebrates in the southeast Pacific: interannual variability and the 1997–1998 El Niño. Limnol Oceanogr 47: 791–802

Paine RT (1976) Size-limited predation: an observational and experimental approach with the *Mytilus-Pisaster* interaction. Ecology 57:858–873

Paine RT (1984) Ecological determinism in the competition for space: the Robert H. MacArthur Award Lecture. Ecology 65:1339–1348

Pakes D, Boulding EG (2010) Changes in the selection differential exerted on a marine snail during the ontogeny of a predatory shore crab. J Evol Biol 23:1613–1622

Pearcy WG, Schoener A (1987) Changes in the marine biota coincident with the 1982–1983 El Niño in the northeastern subarctic Pacific Ocean. J Geophys Res 92: 14417–14428

Peterson CD, Parsons KT, Bethea DM, Driggers WB, Latour RJ (2017) Community interactions and density dependence in the southeast United States coastal shark complex. Mar Ecol Prog Ser 579:81–96

Peterson WT, Fisher JL, Strub PT, Du X, Risien C, Peterson J, Shaw CT (2017) The pelagic ecosystem in the Northern California Current off Oregon during the 2014–2016 warm anomalies within the context of the past 20 years. J Geophys Res Oceans 122:7267–7290

Petraitis PS, Dudgeon SR (2020) Declines over the last two

decades of five intertidal invertebrate species in the western North Atlantic. Commun Biol 3:591
Pfaff MC, Branch GM, Wieters EA, Branch RA, Broitman BR (2011) Upwelling intensity and wave exposure determine recruitment of intertidal mussels and barnacles in the southern Benguela upwelling region. Mar Ecol Prog Ser 425:141–152
Poulin E, Palma AT, Leiva G, Narvaez D, Pacheco R, Navarrete SA, Castilla JC (2002) Avoiding offshore transport of competent larvae during upwelling events: the case of the gastropod *Concholepas concholepas* in Central Chile. Limnol Oceanogr 47:1248–1255
Rasmuson LK, Shanks AL (2020) Revisiting cross-shelf transport of Dungeness crab (*Metacarcinus magister*) megalopae by the internal tide using 16 years of daily abundance data. J Exp Mar Biol Ecol 527:151334
Ray S, Bond N, Siedlecki S, Hermann AJ (2022) Influence of winter subsurface on the following summer variability in Northern California Current System. J Geophys Res Oceans 127:e2022JC018577
Reid DG (1996) The systematics and evolution of *Littorina*. Zoology, Vol 164. Ray Society, London
Reid DG (1990) A cladistic phylogeny of the genus *Littorina* (Gastropoda): implications for evolution of reproductive strategies and for classification. Hydrobiologia 193:1–19
Reid DG, Rumbak E, Thomas RH (1996) DNA, morphology and fossils: phylogeny and evolutionary rates of the gastropod genus *Littorina*. Philos Trans R Soc B 351:877–895
Reid JL Jr, Schwartzlose RA (1962) Direct measurements of the Davidson Current off central California. J Geophys Res 67:2491–2497
Rolán-Alvarez E, Johannesson K, Erlandsson J (1997) The maintenance of a cline in the marine snail *Littorina saxatilis*: the role of home site advantage and hybrid fitness. Evolution 51:1838–1847
Rolán-Alvarez E, Austin C, Boulding EG (2015) The contribution of the genus *Littorina* to the field of evolutionary ecology. Oceanogr Mar Biol Annu Rev 53:157–214
Sanford E, Sones JL, García-Reyes M, Goddard JHR, Largier JL (2019) Widespread shifts in the coastal biota of northern California during the 2014–2016 marine heatwaves. Sci Rep 9:4216
Sergievsky SO, Granovitch AI, Sokolova IM (1997) Long-term studies of *Littorina obtusata* and *Littorina saxatilis* populations in the White Sea. Oceanol Acta 1997:259–265
Shanks AL (1985) Behavioral basis of internal-wave-induced shoreward transport of megalopae of the crab *Pachygrapsus crassipes*. Mar Ecol Prog Ser 24:289–295
Shanks AL (1995) Orientated swimming by megalopae of several eastern North Pacific crab species and its potential role in their onshore migration. J Exp Mar Biol Ecol 186:1–16
Shanks AL, Brink L (2005) Upwelling, downwelling, and cross-shelf transport of bivalve larvae: test of a hypothesis. Mar Ecol Prog Ser 302:1–12
Silva ACF, Mendonça V, Paquete R, Barreiras N, Vinagre C (2015) Habitat provision of barnacle tests for overcrowded periwinkles. Mar Ecol 36:530–540
Sorte CJ, Peterson WT, Morgan CA, Emmett RL (2001) Larval dynamics of the sand crab, *Emerita analoga*, off the central Oregon coast during a strong El Niño period. J Plankton Res 23:939–944
Strathmann RR (2023) Perils of drifting encapsulated embryos of the periwinkle *Littorina scutulata* from failures at launch and unscheduled landings. Mar Ecol Prog Ser 703:109–124
Thomson RE, Krassovski MV (2010) Poleward reach of the California Undercurrent extension. J Geophys Res Oceans 115:C09027
Tolimieri N, Holmes EE, Williams GD, Pacunski R, Lowry D (2017) Population assessment using multivariate time-series analysis: a case study of rockfishes in Puget Sound. Ecol Evol 7:2846–2860
Tseng YH, Ding R, Huang XM (2017) The warm Blob in the northeast Pacific — the bridge leading to the 2015/16 El Niño. Environ Res Lett 12:054019
Underwood AJ, McFadyen KE (1983) Ecology of the intertidal snail *Littorina acutispira* Smith. J Exp Mar Biol Ecol 66:169–197
Wethey DS, Woodin SA (2022) Climate change and *Arenicola marina*: heat waves and the southern limit of an ecosystem engineer. Estuar Coast Shelf Sci 276:108015
Wonham MJ, Hart MW (2018) El Niño range extensions of Pacific Sand Crab (*Emerita analoga*) in the Northeastern Pacific. Northwest Sci 92:53–60
Zaba KD, Rudnick DL, Cornuelle BD, Gopalakrishnan G, Mazloff MR (2020) Volume and heat budgets in the coastal California current system: means, annual cycles, and interannual anomalies of 2014–16. J Phys Oceanogr 50: 1435–1453

Editorial responsibility: Eric Sanford, Bodega Bay, California, USA
Reviewers: This and a previous version reviewed in MEPS by 5 anonymous referees in total
Submitted: April 22, 2024; Accepted: December 9, 2024
Proofs received from author(s): January 26, 2025